JULY 12–16 2020 VIRTUAL JOINT AAPM | COMP MEETING
EASTERN TIME [GMT-4]

Deep-Learning Based Prediction of Physician's Intention for High-Dose-Rate Brachytherapy with Tandem-and-Ovoids Applicator

Y. Gonzalez[1,2], **C. Shen**[1,2], **K. Albuquerque**[1], **X. Jia**[1,2]

[1] Department of Radiation Oncology, University of Texas Southwestern Medical Center, Dallas, Texas, USA

[2] innovative Technology Of Radiotherapy Computations and Hardware Lab, University of Texas Southwestern Medical Center, Dallas, TX, USA

UT Southwestern Medical Center Radiation Oncology

MAIA Laboratory

INTRODUCTION

Treatment planning for radiotherapy is a tedious, time-consuming task that requires a number of iterations between the planner and the physician in order to create plans satisfying the physician's requirements. In an effort to overcome this burden, there has been a number of developments to define metrics to represent physician's preference. However, none of the existing quantitative metrics can fully respects a physician's intention, as the physician's mind can be hardly quantified in a certain mathematical form. Lately, it was believed that a deep neural network can be used represent almost any functions accurately and flexibly. *Driven by this idea, in this work, we developed a deep-learning based method that learns physician's intention and incorporates it into dose prediction for high-dose-rate brachytherapy (HDRBT).*

To our knowledge, this is the first time that a deep learning framework was developed to represent physician's intention when deciding to accept or reject a plan. This was made possible by using the state-of-the-art deep neural networks that can be used to represent functions accurately and flexibly and by an innovative network training process. *The methodology of this tool can be potentially generated to other sites and technologies to provide guidance for different treatment planning applications.*

METHOD

Overview

The system consisted of a dose prediction networks (DPN) and preference prediction network (PPN). DPN predicts EQD2 of OAR D2cc and CTV D90 from patient 3D anatomy. PPN reflects a physician's intention by outputting the probability of a given plan being acceptable to the physician based on the patient's anatomy. Network training was performed first through individual training, followed by joint DPN-PPN training. We collected approved treatment plans of 228 treatment fractions from 64 patients. Among them, 200 plans from 57 patients was employed as training and the remaining 28 plans from other 7 patients were saved for testing.

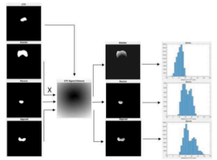

Fig. 1. Method of converting binary contours to distance histograms.

Data Pre-Processing

We obtained physician contours of patient anatomy that were delineated during patient treatment. All contours and plan information were exported from Eclipse Treatment Planning System in DICOM-RT format then processed into binary images in MATLAB. Binary contour volumes were resampled from 1.1719 mm x 1.1719 mm x 2 mm resolution to 1 mm x 1 mm x 1 mm resolution. Patient OAR binary contours (bladder, rectum, and sigmoid) were converted to a distance from CTV boundary map and the CTV binary contour was converted into a distance from source map. OAR and CV distance maps were then converted in distance histograms (Fig. 1).

Network Individual Training

In individual training, DPN was trained to output clinical dose distributions, while PPN was trained to differentiate clinical plans from those generated by randomly perturbing dwell times of corresponding clinical plans.

Network structures can be seen in Fig. 2. This step provided good initializations for the next step. Loss functions for DPN and PPN are shown in Eq. (1) and Eq. (2), respectively, over a training data set, Tr, where A is the patient anatomy represented by the distance histograms, P is a given plan defined by OAR and CTV EQD2, and Y is the label of "acceptable" (value of 1) or "unacceptable" (value of 0) for a given plan. Unacceptable plans, in addition to those plans that exceed clinical constraints, also include plans that satisfy these planning goals but are infeasible in practice.

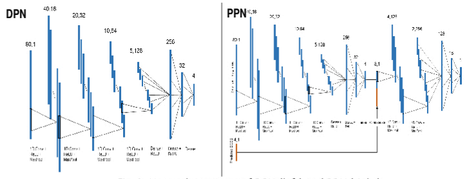

Fig. 2. Network structure of DPN (left) and PPN (right).

$$\min_{\theta} E_{t\in Tr}\left[\|DPN(P,A|\theta) - Y\|_2^2\right] \quad \text{Eq. (1)}$$

$$\min_{\theta} E_{t\in Tr}\left[\|PPN(A|\theta) - Clinical\ EQD2\|_2^2\right] \quad \text{Eq. (2)}$$

Network Joint Training

In the second step of joint training, two network models were simultaneously fine tuned via an adversarial process as seen in Fig. 3.

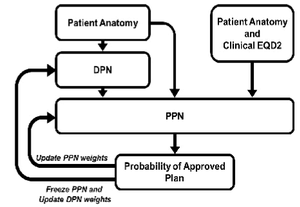

Fig. 3. Joint training procedure between DPN and PPN

More specifically, the network parameters in DPN and PPN were trained alternatively in an adversarial fashion.

In each training iteration, network parameters of PPN were updated by solving the optimization problem in Eq. (3) with DPN being frozen. PPN was then fixed and DPN was trained by solving the optimization problem in Eq. (4). By using this framework, PPN was able to continue learning beyond the limited dataset available through independent training with new data generated by DPN at each epoch. This adversarial process not only refined PPN on learning the physician's intention, but also incorporated it as a guidance to train DPN for more accurate EQD2 prediction.

$$\min_{\theta_{PPN}} E_{t\in Tr}\left[\|PPN(Clinical\ EQD2, A|\theta_{PPN}) - 1\|_2^2 + \|PPN(DPN(A|\theta_{DPN}), A)|\theta_{PPN})\|_2^2\right] \quad \text{Eq. (3)}$$

$$\min_{\theta_{DPN}} E_{t\in Tr}\left[\|PPN(DPN(A|\theta_{DPN}), A)|\theta_{PPN}) - 1\|_2^2 + \lambda\|PPN(A|\theta_{PPN}) - Clinical\ EQD2\|_2^2\right] \quad \text{Eq. (4)}$$

RESULTS

After joint training, the models were evaluated on their ability to predict a physician's preference for a given plan. DPN accuracy was quantified using relative error. PPN model was evaluated 6 times for every testing fraction. the 6 testing samples come from: clinically approved EQD2, DPN-predicted EQD2, increasing DPN prediction twice between 10% and 15%, and decreasing DPN prediction twice between 10% and 15%. Results were quantified via sensitivity, specificity, and AUC.

DPN Results

After training, we evaluated the DPN ability to predict patient EQD2. *More specifically, this prediction error was calculated to be 8% ± 7.5%, 8.8% ± 5.9%, 7.2% ± 6.2%, and 6.9% ± 4.8% across the bladder, rectum, sigmoid, and CTV, respectively.* Results for the 28 testing fractions are shown in Fig. 4.

PPN Results

For a given testing fraction, after applying the threshold, we found that the DPN was able to differentiate between "acceptable" and "unacceptable" plans 9% from the clinical plan with 90% accuracy, and a sensitivity and specificity of 0.88 and 0.85, respectively. Results are shown in Fig. 5.

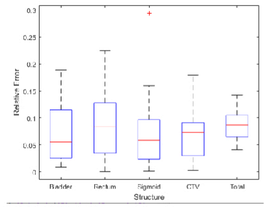

Fig. 4. DPN individual structure and overall OAR relative error. Central red mark indicated median, top and bottom edges of box indicated 75th and 25th percentiles, respectively.

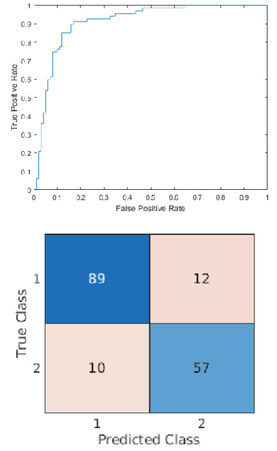

Fig. 5. ROC curve (left) and confusion matrix and predicted class (right). In the confusion matrix, class of "1" represent unacceptable plans and class of "2" represent acceptable plans.

CONCLUSION

Through a combination of individual and joint training, we were able to develop two models: (1) a DPN that predicts patient-specific dose for a given fraction, and (2) a PPN that predicts the physician's intention for a given plan based on patient anatomy. Both the DPN and PPN models were evaluated on the same 28 independent testing fractions from HDRBT treatment planning for cervical cancer. We found that under this novel framework, DPN can accurately predict anatomy-specific clinical EQD2 and PPN was able to learn the physician's preference for a given plan based on patient-specific anatomy.

CONTACT INFORMATION

Email: yeseniaa.gonzalez@utsouthwestern.edu